

Rapid synthesis and turnover of brain microsomal ether phospholipids in the adult rat

Thad A. Rosenberger,¹ Jun Oki, A. David Purdon, Stanley I. Rapoport, and Eric J. Murphy

Brain Physiology and Metabolism Section, National Institute on Aging, National Institutes of Health, Building 10, Room 6N202, Bethesda, MD 20892-1582

Abstract The rates of synthesis, turnover, and half-lives were determined for brain microsomal ether phospholipids in the awake adult unanesthetized rat. A multicompartamental kinetic model of phospholipid metabolism, based on known pathways of synthesis, was applied to data generated by a 5 min intravenous infusion of [1,1-³H]hexadecanol. At 2 h post-infusion, 29%, 33%, and 31% of the total labeled brain phospholipid was found in the 1-*O*-alkyl-2-acyl-*sn*-glycero-3-phosphate, ethanolamine, and choline ether phospholipid fractions, respectively. Autoradiography and membrane fractionation showed that 3% of the net incorporated radiotracer was in myelin at 2 h, compared to 97% in gray matter microsomal and synaptosomal fractions. Based on evidence that ether phospholipid synthesis occurs in the microsomal membrane fraction, we calculated the synthesis rates of plasmalycholine, plasmanylethanolamine, plasmanylethanolamine, and plasmanylcholine equal to 1.2, 9.3, 27.6, and 21.5 nmol·g⁻¹·min⁻¹, respectively. Therefore, 8% of the total brain ether phospholipids have half-lives of about 36.5, 26.7, 23.1, and 15.1 min, respectively. Furthermore, we clearly demonstrate that there are at least two pools of ether phospholipids in the adult rat brain. One is the static myelin pool with a slow rate of tracer incorporation and the other is a dynamic pool found in gray matter. The short half-lives of microsomal ether phospholipids and the rapid transfer to synaptosomes are consistent with evidence of the marked involvement of these lipids in brain signal transduction and synaptic function.—Rosenberger, T. A., J. Oki, A. D. Purdon, S. I. Rapoport, and E. J. Murphy. Rapid synthesis and turnover of brain microsomal ether phospholipids in the adult rat. *J. Lipid Res.* 2002. 43: 59–68.

Supplementary key words brain • plasmalogen • hexadecanol • autoradiography • myelin • half-life • synapses • synaptosome • peroxisome • microsome

Ether phospholipids are naturally occurring lipids having either a 1-*O*-alkyl (plasmanyl) or a 1-*O*-alk-1'-enyl (plasmenyl) linkage at the *sn*-1 position of the glycerol backbone. In mammalian cells, these lipids belong almost exclusively to the choline and ethanolamine glycerophospholipid classes (1) and are especially abundant in the heart, kidney, and central nervous system (CNS) (2–4). In

the human brain, plasmenyl-type ether phospholipids (plasmalogens) compose approximately 23% of total brain phospholipids (2) while in the rat brain and monkey spinal cord, 33% to 35% of myelin phospholipids are plasmalogens (5, 6). Although the large proportion of ether phospholipids within the central nervous system implies a structural role, evidence exists that suggests important physiological functions.

For example, the mammalian brain contains anabolic acyltransferases, phosphotransferases (7, 8), and catabolic lipases (9–12) that are selective for plasmanyl and plasmenyl-type phospholipids. A 39 kDa phospholipase A₂ (PLA₂) has been found in the brain that is highly selective for plasmenylethanolamine (PlsEtn) and may be involved in both plasmalogen acyl chain remodeling and arachidonate release (13). The brain also contains microsomal enzymes that metabolize 2-lysoplasmenylethanolamine produced by the 39 kDa PLA₂, forming ethanolamine or phosphoethanolamine (9). These enzymes degrade 2-lysoplasmenylethanolamine in a similar fashion (14). Platelet activating factor, an ether phospholipid, is also synthesized in the brain and is involved in CNS function (15) and signal transduction (16). Collectively, the presence of these enzymes in the brain suggests that the substrate phospholipids and their metabolites have an important

Abbreviations: ChoGpl, choline glycerophospholipids; DHAP, dihydroxyacetonephosphate; EtnGpl, ethanolamine glycerophospholipids; 16:0(ol), hexadecanol; alkyl-DHAP, 1-*O*-alkyl-dihydroxyacetone phosphate; 2-lyso-PakOH, 1-*O*-alkyl-2-lyso-*sn*-glycero-3-phosphate; FFA, free fatty acid; HOGpl, diradyl-*sn*-glycerol-3-phosphate; 2-lysoPakCho, 2-lysoplasmanylcholine (1-*O*-alkyl-2-lyso-*sn*-glycero-3-phosphocholine); 2-lysoPlsCho, 2-lysoplasmenylcholine (1-*O*-alk-1'-enyl-2-lyso-*sn*-glycero-3-phosphocholine); 2-lysoPakEtn, 2-lysoplasmanylethanolamine (1-*O*-alkyl-2-lyso-*sn*-glycero-3-phosphoethanolamine); 2-lysoPlsEtn, 2-lysoplasmenylethanolamine (1-*O*-alk-1'-enyl-2-lyso-*sn*-glycero-3-phosphoethanolamine); PakCho, plasmanylcholine (1-*O*-alkyl-2-acyl-*sn*-glycero-3-phosphocholine); PakEtn, plasmanylethanolamine (1-*O*-alkyl-2-acyl-*sn*-glycero-3-phosphoethanolamine); PakOH, 1-*O*-alkyl-2-acyl-*sn*-glycero-3-phosphate; PlsCho, plasmenylcholine (1-*O*-alk-1'-enyl-2-acyl-*sn*-glycero-3-phosphocholine); PlsEtn, plasmenylethanolamine (1-*O*-alk-1'-enyl-2-acyl-*sn*-glycero-3-phosphoethanolamine).

¹ To whom correspondence should be addressed.
e-mail: plsetn@mail.nih.gov

biological function. In this regard PlsEtn promotes membrane fusion and vesicle formation (17) suggesting a potential role in membrane trafficking (18). Ether phospholipids are also a reservoir of arachidonate, (19) and the high reactivity of the vinyl ether linkage with singlet oxygen and reactive oxygen species suggests that plasmalogens may serve as potential membrane localized antioxidants (20).

Ether phospholipids in the brain are synthesized in peroxisomes and microsomes (21, 22) and are then transferred to synaptic membranes or to myelin (18, 23–25). Added to the evidence that ether phospholipids participate in a large number of metabolic processes, such transfer suggests that they likely play an active role in signal transduction and synaptic activity. Nevertheless, measurements of decay half-lives of ether phospholipids, following their labeling by intracerebral injection of [^{14}C]ethanolamine, [^3H]glycerol, [^{14}C]choline, and [^{32}P]phosphate, indicate half-lives of 11 to 58 days in myelin and microsomal lipids, 30 days in whole brain, and 6 and 9.5 days in neurons and glia, respectively (26, 27). On the other hand, consistent with a more dynamic role, is the rapid accumulation of radioactivity into brain ether phospholipids within 1 to 4 h after intracerebral injection of these precursors. Thus, using standard tracer incorporation equations (28), Masuzawa et al. (29) showed that intracerebrally injected [$1\text{-}^3\text{H}$]glycerol in myelinating rats gave a rate of synthesis of PlsEtn equal to $32 \text{ nmol} \cdot \text{g}^{-1} \cdot \text{min}^{-1}$, equivalent to a turnover rate of 5.3% per h and a half-life of 13 h. This suggests that the biosynthetic reactions involved in the incorporation of the tracer into the phospholipid fractions occur at a more rapid rate than efflux calculations demonstrate. However, the long half-lives calculated from classic efflux experiments appear excessive and likely reflect the brain's ability to recycle the tracer as well as reflecting the dilution of labeled phospholipids into metabolically inactive membranes (27, 30, 31). Furthermore, if synthesis takes place in only a small, rapidly turning over brain phospholipid pool (21, 22), this fact should be taken into account when estimating turnover and half-lives. This has not been the case in prior in vivo studies.

Therefore, to assess the possibility that ether phospholipids are rapidly metabolized in the brain, rates of synthesis, turnover, and half-lives of microsomal brain ether phospholipids were measured based on known pathways of synthesis. In these experiments, [$1,1\text{-}^3\text{H}$]hexadecanol was infused intravenously in the awake rat, and its incorporation into different brain ether phospholipid compartments was quantified as a function of time by both analytical and quantitative autoradiographic techniques. Since the enzyme catalyzing the first committed step in ether phospholipid synthesis, alkyl-DHAP synthase, is not selective toward fatty alcohols of chain lengths between C_{10} and C_{22} (32), [$1,1\text{-}^3\text{H}$]hexadecanol was used as a representative substrate for this enzyme and for the subsequent reactions outlined in Fig. 1. Also, the use of [$1,1\text{-}^3\text{H}$]hexadecanol permits measurement of only ether phospholipid synthesis because the tritium atoms are lost during the oxidation of [$1,1\text{-}^3\text{H}$]hexadecanol to palmitate. Furthermore,

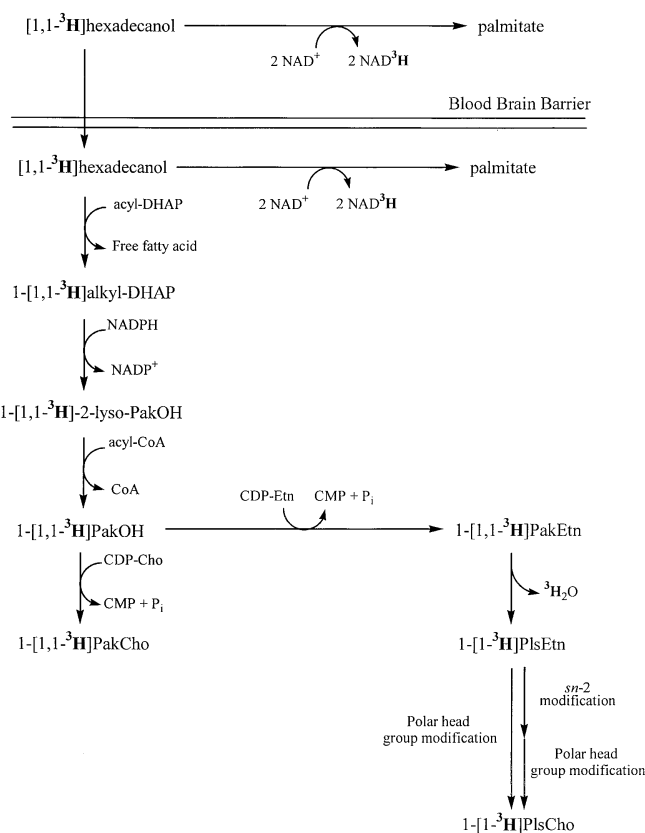


Fig. 1. Pathways of ether phospholipid biosynthesis showing the reactive brain ether phospholipid pools and the flow of the tritium label following the intravenous infusion of [$1,1\text{-}^3\text{H}$]hexadecanol. After [$1,1\text{-}^3\text{H}$]hexadecanol enters brain, oxidation to palmitate results in the loss of [^3H] atoms. The initial steps of biosynthesis involve the formation of a fatty alcohol and acyl-dihydroxyacetone phosphate (acyl-DHAP) in the peroxisomes. These reactions are catalyzed by acyl-CoA reductase and DHAP acyltransferase. Alkyl-DHAP synthase then catalyzes the condensation of fatty alcohol with acyl-DHAP to produce alkyl-DHAP and free fatty acid. Alkyl-DHAP is then reduced on the cytoplasmic side of the peroxisome by alkyl-DHAP reductase forming 2-lysoPakOH. 2-lysoPakOH is transferred to microsomes, where it is acylated at the *sn*-2 position, dephosphorylated, and converted to PakCho or PakEtn by 1-*O*-alkyl-2-lyso-*sn*-glycerol-3-phosphate acyltransferase, 1-*O*-alkyl-2-acyl-*sn*-glycerol-3-phosphate phosphohydrolase, and 1-*O*-alkyl-2-acyl-*sn*-glycerol: CDP-choline choline (CDP-ethanolamine ethanolamine) phosphotransferases, respectively. The formation of plasmalogen-type glycerophospholipids is initiated by insertion of a *cis*-double bond between C_1 and C_2 of the fatty alcohol at the *sn*-1 position of PakEtn, and is catalyzed by the $\Delta 1$ alkyl desaturase complex. The formation of choline plasmalogen is preceded by the formation of PakEtn and PlsEtn. One ^3H atom is lost in the conversion of [$1,1\text{-}^3\text{H}$]hexadecanol-labeled PakEtn to PlsEtn. PlsCho if formed from PlsEtn by either direct polar head-group modification or by *sn*-2 modification followed by polar head-group modification. Once the ether phospholipids are formed, they are transferred from microsomal to synaptic membranes (21, 22).

there is stoichiometric retention of the label following the desaturation step involved in plasmalogen formation allowing for the quantitative measure of plasmalogen biosynthesis. This combined approach allows us to determine the distribution of the tracer following infusion, and estimate the rate at which these phospholipids turnover by

calculating the flux of the tracer through the microsomal ether phospholipid pool. We report here, for the first time, synthesis rates, turnover times, and half-lives of brain microsomal ethanolamine and choline ether phospholipids *in vivo*, and show that in the adult rat the tracer is preferentially incorporated into gray matter regions. We also present an animal model in which ether phospholipid function in the post-myelinating rat can be assessed.

MATERIALS AND METHODS

[1,1-³H]hexadecanol (55 Ci · mmol⁻¹ ≥97% pure) was purchased from Moravek Biochemicals (Brea, CA). Phospholipid and neutral lipid standards were from Nu-Chek-Prep (Elysian, MN) and fatty alcohol standards and “essentially fatty acid free” bovine serum albumin was from Sigma Chemical Co. (St. Louis, MO). Acetic anhydride, anhydrous pyridine, and thin-layer chromatography plates were from Analtech (Deerfield, IL). High performance liquid chromatography grade *n*-hexane and 2-propanol were from EM Science (Gibbstown, NJ). Reagent grade chloroform, methanol, and other chemicals were from Mallinckrodt (Paris, KY) unless noted otherwise. Scintillation cocktail (Beckman Ready-Safe, Fullerton, CA) containing 1% glacial acetic acid was used to determine radioactivity in all samples. Extracts were stored in *n*-hexane: 2-propanol (3:2, v/v) + 5.5% H₂O under N₂ at -20°C unless otherwise noted.

Surgery was performed, as previously described (33), in accordance with NIH guidelines (NIH Publication no. 80-23). Briefly, a 3-month-old male Sprague-Dawley rat, weighing 150–280 g (Charles River, Wilmington, MA), was anesthetized with 2% to 3% halothane (Halocarbon, River Edge, NJ). Polyethylene catheters (PE 50, Becton Dickinson, Sparks, MD) filled with 100 IU sodium heparin were tied into the right femoral artery and vein. The skin was closed with clips and 1% lidocaine was applied as a local anesthetic. The animal was wrapped loosely in a fast-setting plaster body cast, taped to a wooden block, and allowed to recover from anesthesia for at least 3 h. Body temperature was maintained at 36.5°C using a rectal probe and a feedback-heating device (Yellow Springs Laboratories, Yellow Springs, OH).

Using an infusion pump (Harvard Apparatus, South Natick, MA) an awake rat was infused intravenously for 5 min at a rate of 0.4 ml · min⁻¹ with isotonic saline containing 1.75 mCi · kg body wt⁻¹ [1,1-³H]hexadecanol suspended in 0.06 mg bovine serum albumin. Arterial samples were collected during and following the infusion to determine the radioactivity and levels of unlabeled lipids in whole blood and plasma. At fixed times between 5 and 240 min following the start of infusion, the rat was killed by sodium pentobarbital (100 mg · kg body wt⁻¹, i.v.). Animals used to analyze whole brain lipids were subjected to head-focused microwave irradiation (5.5 kw, 3.4 s, Cober Electronics, Stamford, CT). All brains were immediately excised, frozen on dry ice, and stored at -80°C.

To isolate different brain fractions, frozen brain was dispersed using a glass Tenbroeck homogenizer in 50 mM Tris buffer, pH 7.5, containing 0.32 M sucrose. Frozen brain has been studied previously in this manner (34). Myelin and gray matter membranes (microsomes and synaptosomes) were separated using continuous sucrose density centrifugation as described previously (24). Myelin fractions were purified by osmotic shock, resuspension, and washing with water to remove the sucrose. Fractions obtained in this way have been characterized by electron microscopy, enzymic assay, and lipid analysis (5, 35–39). With regard to lipid analysis, the phospholipid content of each of our fractions was comparable to published values (1, 24).

Regional brain radioactivity was determined at 30, 60, and 240 min following the start of infusion by quantitative autoradiography (40). Frozen brains were secured to mounts with embedding media and cut into 20-μm coronal sections at -20°C in a cryostat (Model OTF, Bright Instruments, Huntington, England). The sections were placed on glass cover slips and dried at 60°C to 70°C for 45 min. Dry slides were attached to boards, inserted into film cassettes beside radioactive tissue standards (Amersham Corp., Arlington Heights, IL), and exposed for 20 weeks. The films were developed, fixed, and analyzed. Regional brain radioactivity was measured in sextuplet by digital quantitative densitometry using NIH Image (Version 1.55, created by Wayne Rasband, NIH).

The whole brain was weighed and extracted as previously described (33). Samples of plasma, blood, and membrane fractionations were extracted using the Folch method (41). The extracts were concentrated *in vacuo* (Savant, Hickville, NY), dissolved in *n*-hexane [2-propanol (3:2, v/v) + 5.5% H₂O] and filtered using a 0.2 μm nylon filter.

Standards and samples were applied to 20 cm × 20 cm Whatman silica gel 60A LK6 TLC plates and separated as previously described (42). Bands corresponding to ethanolamine (EtnGpl) and choline glycerophospholipid (ChoGpl), diradyl-*sn*-glycerol-3-phosphate (HOGpl), and neutral lipids were scraped from TLC plates stored. EtnGpl and ChoGpl fractions were extracted from the silica gel using *n*-hexane [2-propanol (3:2, v/v) + 5.5% H₂O] and concentrated with N₂ at 40°C. Samples were incubated in 2 ml methanol containing 0.1 M of [KOH]hydroxide of potassium hydrate at 30°C for 15 min to cleave the acyl chains. At 15 min, 1 ml methyl formate (Sigma Chemical Co., St. Louis, MO) was added followed by 4 ml chloroform [*n*-butanol (4:2, v/v)]. Adding 2 ml 0.1 M KCl formed two phases and their separation was promoted by centrifugation at 1000 × g (43). The lower solvent phase, containing the lyso-ether phospholipid analogs 1-*O*-alkyl-2-lyso-*sn*-glycerol-3-phosphoethanolamine (2-lysoPakEtn) + 1-*O*-alk-1'-enyl-2-lyso-*sn*-glycerol-3-phosphoethanolamine (2-lysoPlsEtn) or 1-*O*-alkyl-2-lyso-*sn*-glycerol-3-phosphocholine (2-lysoPakCho) + 1-*O*-alk-1'-enyl-2-lyso-*sn*-glycerol-3-phosphocholine (2-lysoPlsCho), were retained. The extracts were concentrated with N₂ at 40°C and dissolved in chloroform. Aliquots of each sample were spotted onto two 10 cm × 10 cm silica gel G TLC plates (Analtech, Deerfield, IL), and the lipid classes were separated using chloroform-methanol-ammonium hydroxide (65:25:4, v/v/v). The second TLC plates were exposed to HCl fumes for 15 min before separation using the solvent system described above. Bands corresponding to 2-lysoPakEtn + 2-lysoPlsEtn, and 2-lysoPakCho + 2-lysoPlsCho (plate #1) or 2-lysoPakEtn, and 2-lysoPakCho (plate #2) were scraped from the TLC plates and transferred to acid-washed 16 mm × 120 mm test tubes. A portion of the sample was used to quantitate radioactivity, while the remainder was assayed for lipid phosphorus (44).

Neutral lipids and brain HOGpl from the phospholipid separation were extracted from the silica gel using *n*-hexane [2-propanol (3:2, v/v) + 5.5% H₂O]. Brain neutral lipids, plasma, and whole blood lipid extracts were concentrated with N₂ at 40°C and dissolved in chloroform. Samples and standards were applied to 20 cm × 20 cm Analtech silica gel G TLC plates and the neutral lipids separated as previously described (45). Bands corresponding to fatty alcohol (brain or plasma) or to HOGpl (brain) were transferred to separate acid washed tubes and dissolved in *n*-hexane [2-propanol (3:2, v/v) + 5.5% H₂O]. Liquid scintillation counting quantitated radioactivity and the specific activity was determined by assaying for lipid phosphorus (44) following methanolic KOH hydrolysis of the HOGpl and separation via TLC, as described above. The fatty alcohol was quanti-

tated following acetate derivatization by gas liquid chromatography (GLC). GLC of acetate derivatives from brain, whole blood, and plasma fatty alcohols were separated using a gas chromatograph (Model 5890, series II, Hewlett-Packard, King of Prussia, PA) equipped with a capillary column (SP 2330; 30 m × 0.32 mm i.d., Supelco, Bellefonte, PA) and a flame ionization detector.

Theory and calculations

The equations that we applied to our data are based on known pathways of brain ether phospholipid biosynthesis (Fig. 1) and on evidence that ether phospholipid synthesis occurs in brain peroxisomes and microsomes (microsomal fraction) (21, 22). The radioactivity (dpm · gram⁻¹) of hexadecanol and of the different ether phospholipids was measured in plasma and whole brain extracts of rats killed at 5, 10, 20, 30, 60, or 120 min following the start of infusion. Parenchymal brain radioactivity in each pool *i*, $c_{br,i}^*$ (dpm · ml⁻¹) was then calculated by subtracting the intravascular contribution for that compound from its net brain radioactivity. Intravascular radioactivity was taken as the compound's radioactivity (dpm · ml⁻¹) in whole blood at the time of brain sampling and multiplied by the brain blood volume (0.023 ml · g brain⁻¹) (46).

The radioactivity of plasma hexadecanol ($c_{pl,hex}^*$), brain hexadecanol, and ether phospholipids [$c_{br,i}^*(T_2)$] was used to calculate the integrated compartmental radioactivity from the beginning of infusion at time 0 to the time of brain sampling

$$T_2 \int_0^{T_2} c_{br,i}^* dt$$

using the trapezoidal rule (SigmaPlot Windows, Version 5.0, SPSS, Chicago, IL). The unidirectional transfer coefficient ($k_{i-1 \rightarrow i}^*$, equation 1) for transfer of labeled hexadecanol from a substrate compartment (*i* - 1) to product compartment (*i*) was calculated as the ratio of the brain radioactivity $c_{br,i}^*(T_2)$ in *i* to the integrated radioactivity of *i* - 1 between T_1 and T_2 .

$$dc_{br,i}^*/dt = k_{i-1 \rightarrow i}^* c_{br,i-1}^* \quad (Eq. 1)$$

T_1 and T_2 were chosen to cover the period of the linear rate of change of radioactivity in *i*, when radioactivity essentially reflected synthesis de novo. Specific equations of the form in equation 1 can be written on the basis of the pathways outlined in Fig. 1. For PakOH, PakCho, PakEtn, PlsEtn, and PlsCho these equations are:

$$dc_{br,PakOH}^*/dt = k_{hex \rightarrow PakOH}^* c_{br,hex}^* \quad (Eq. 1a)$$

$$dc_{br,PakCho}^*/dt = k_{PakOH \rightarrow PakCho}^* c_{br,PakOH}^* \quad (Eq. 1b)$$

$$dc_{br,PakEtn}^*/dt = k_{PakOH \rightarrow PakEtn}^* c_{br,PakOH}^* \quad (Eq. 1c)$$

$$dc_{br,PlsEtn}^*/dt = k_{PakEtn \rightarrow PlsEtn}^* 2(c_{br,PakEtn}^*) \quad (Eq. 1d)$$

$$dc_{br,PlsCho}^*/dt = k_{PlsEtn \rightarrow PlsCho}^* c_{br,PlsEtn}^* \quad (Eq. 1e)$$

Therefore, T_1 and T_2 were taken at 0 and 5 min for hexadecanol, and at 0 and 30 min for the different brain ether phospholipids.

The transfer coefficient ($k_{i-1 \rightarrow i}^*$), in units of time⁻¹, is independent of mass (equation 1). Therefore, to calculate mass flux or the rate of synthesis from *i* - 1 to *i* using this coefficient $k_{i-1 \rightarrow i}^*$ must be multiplied by the unlabeled concentration of *i* - 1 (nmol · g⁻¹) in the brain pool in which synthesis of *i* takes place, namely the peroxisomal-microsomal brain fraction (equation 2). $c_{br,i-1}$ is the unlabeled concentration of *i* in the microsomal brain fraction (equation 2).

$$J_{i-1 \rightarrow i} = k_{i-1 \rightarrow i}^* c_{br,i-1} \quad (Eq. 2)$$

Treating these reactions as first order, we divided $J_{i-1 \rightarrow i}$ by the microsomal concentration of *i*, ($c_{br,i}$) to estimate the turnover rate of *i* (equation 3), from which its half-life, ($t_{1/2,i}$), can be estimated (equation 4) (47, 48).

$$F_i = J_{i-1 \rightarrow i} / c_{br,i} \quad (Eq. 3)$$

$$t_{1/2,i} = 0.693 / F_i \quad (Eq. 4)$$

Steady state constraints

Our study was performed at steady state, defined as the condition in which the unlabeled concentrations of brain ether phospholipids do not change with time. For the biosynthetic pathways outlined in Fig. 1, at steady state the synthesis rate of *i* from its precursor equals the rate of conversion of *i* to its products (28, 49). This type of analysis provides two additional constraints to the model. The constraints are that the rate of synthesis of PakCho and PakEtn must equal the rate of synthesis of PakOH (Equation 5) and that the rates of synthesis of PakEtn, PlsEtn, and PlsCho should be equal (equation 6).

$$J_{hex \rightarrow PakOH} = J_{PakOH \rightarrow PakCho} + J_{PakOH \rightarrow PakEtn} \quad (Eq. 5)$$

$$J_{PakOH \rightarrow PakEtn} = J_{PakEtn \rightarrow PlsEtn} = J_{PlsEtn \rightarrow PlsCho} \quad (Eq. 6)$$

Therefore, both equations five and six must hold to the extent that the assumption of steady state is valid. These assumptions and the recognition that synthesis of ether phospholipids occur in the peroxisomes and microsomes (microsomal fraction) by reactions outlined in Fig. 1 allows us to estimate the transfer coefficients of the tracer into the stable ether phospholipids, then use these coefficients to calculate the rates at which the microsomal ether phospholipids are synthesized and turnover.

RESULTS

As illustrated in Fig. 2, both plasma (Fig. 2, inset) and whole blood organic phase radioactivity rose during the 5 min of intravenous infusion of [1,1-³H]hexadecanol in the awake adult rat. Following infusion, plasma radioactivity declined with a half-life of 1.8 min ± 0.3 min (n = 5). Radioactivity in volatile aqueous extracts (not shown) due to [³H]H₂O produced by peripheral and central metabolism of injected [1,1-³H]hexadecanol, increased to 30 min and then remained essentially unchanged to 120 min. The plasma and whole blood extracts contained mainly [1,1-³H]-hexadecanol, with small amounts of radioactive ether phospholipids and diradylglycerol (data not shown).

Trace amounts of radioactivity were found in the phosphatidyl fractions of blood and brain phospholipid, confirming the complete loss of the tritium atoms due to oxidation of [1,1-³H]hexadecanol to palmitate (50). As illustrated in Fig. 3A and B, the time course of increasing brain [1,1-³H]hexadecanol largely reflected the increase of whole blood or plasma radioactivity, indicating a rapid exchange of the tracer across the blood-brain barrier. Following the 5 min infusion, however, brain [1,1-³H]hexadecanol declined more slowly than did the tracer in whole blood or plasma, reflecting the high octanol-water partition coefficient (log P_{hex} = 4.81) (51), which accounts for its rapid diffusion across the blood brain barrier, high lipid solubility, and retention of the tracer within membrane lipids (52).

Brain PakOH radioactivity peaked at 5 min after the start of infusion and remained essentially constant thereafter (Fig. 3A). Radioactivity in each of the two metabolic products of PakOH, PakCho, and PakEtn (Fig. 3B), increased roughly linearly between 5 min and 30 min, as did

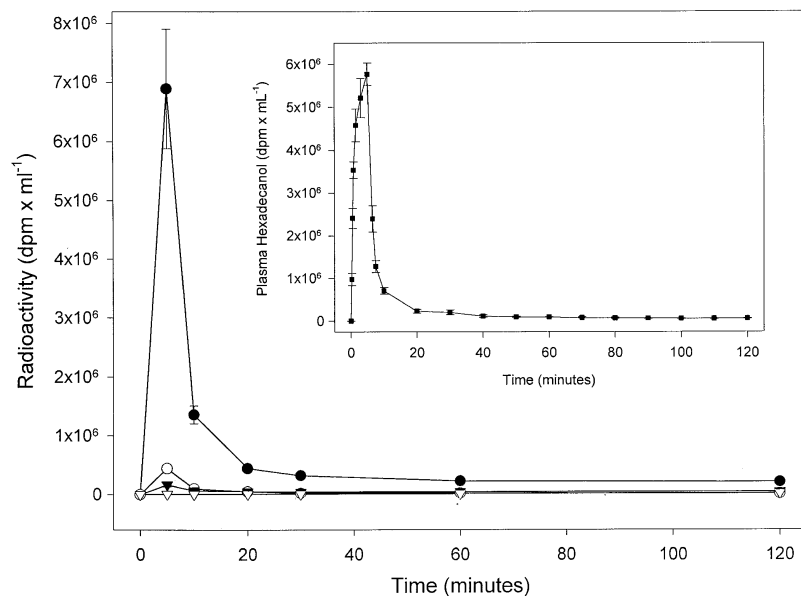


Fig. 2. Time course of whole blood and plasma radioactivity in Folch organic extracts with 5 min of intravenous infusion of $1.75 \text{ mCi} \cdot \text{kg}^{-1}$ $[1,1\text{-}^3\text{H}]$ -hexadecanol. Symbols represent: whole blood hexadecanol, solid circles; whole blood PakOH, open circles; whole blood PlsEtn, solid triangles; whole blood PlsCho, open triangles; plasma hexadecanol, solid squares (figure inset). Values are means \pm SD ($n = 5$).

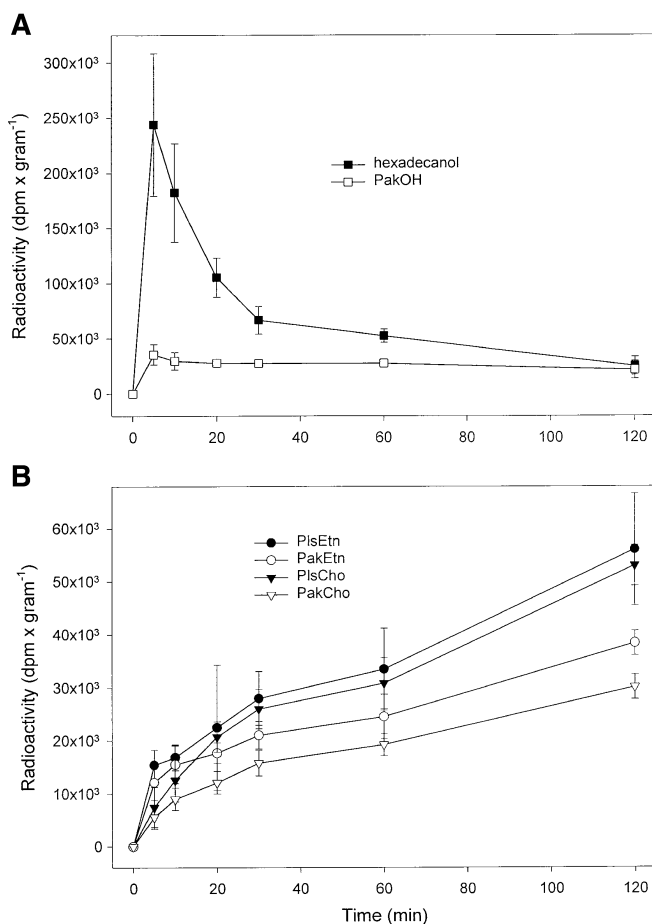


Fig. 3. Time course of radioactivity in brain ether phospholipids, with 5 min of intravenous infusion of $1.75 \text{ mCi} \cdot \text{kg}^{-1}$ $[1,1\text{-}^3\text{H}]$ hexadecanol. A: Labeled hexadecanol and 1-*O*-alkyl-2-acyl-*sn*-glycerol-3-phosphate (PakOH). B: Labeled plasmalycholine (PakCho), plasmylethanolamine (PakEtn), plasmylethanolamine (PlsEtn), and plasmylethanolamine (PlsCho). Values are means \pm SD ($n = 5$), corrected for intravascular radioactivity.

the radioactivity in the later products, PlsEtn and PlsCho (Fig. 3B).

Representative autoradiographs of coronal brain sections at 240 min following the intravenous infusion of $[1,1\text{-}^3\text{H}]$ hexadecanol are illustrated in **Fig. 4**. Radioactivity was much greater in gray than white matter regions, and very high in the choroid plexus and cerebral ventricles. **Table 1** summarizes data from the serial autoradiographs taken at 30, 60, and 240 min following the start of infusion. Comparison of the absolute values for radioactivity ($\text{dpm} \cdot \text{gram}^{-1}$) shows that radioactivity increased or did not change between 30 and 240 min in gray matter regions, but declined by a factor of three in white matter regions. Greater radioactivity was found in gray than white matter regions at 60 min, whereas at 240 min, gray to white matter ratios of radioactivity were as high as 6:1.

Membrane fractionation

Clearly, the autoradiographic studies indicate that at later times there is a lack of labeling in the white matter, suggesting a difference between the myelin plasmalogen pool and plasmalogen found elsewhere in the brain. To further characterize this spatial and perhaps chemical heterogeneity, the brain myelin and membranes were fractionated and ether phospholipid radioactivity quantified biochemically. As evident in **Table 2**, the decline in net white matter radioactivity between 30 and 240 min largely reflected the loss of unincorporated $[1,1\text{-}^3\text{H}]$ hexadecanol. Excluding unincorporated $[1,1\text{-}^3\text{H}]$ hexadecanol, it is evident that the myelin fraction contained less than 10% of net lipid incorporated radioactivity between 30 and 240 min, and less than 3% at 240 min. Greater than 97% of the incorporated radioactivity at 240 min was within the brain microsomal and synaptosomal fractions. These numbers further substantiate the chemical and spatial heterogeneity found in the adult rat brain under these experimental conditions.

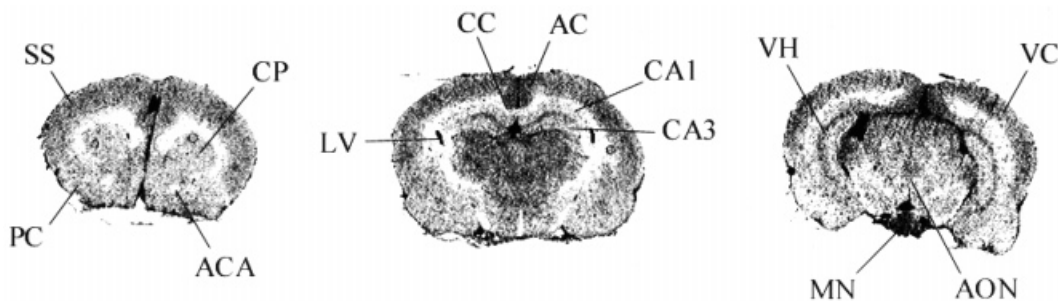


Fig. 4. Representative autoradiograph of coronal sections of rat brains at 240 min following the start of the 5 min infusion of [1,1-³H]hexadecanol. Different brain sections are shown to indicate the pattern of incorporation in different regions. Distance from bregma: Left, 1.70 mm; middle, -3.14 mm; right, -4.80 mm. Abbreviations not defined in text: SS, somatosensory cortex; PC, pyriform cortex; ACA, anterior commissure, anterior; CC, corpus callosum; CP, caudate putamen; LV, lateral ventricle; CA1, CA1 region hippocampus; CA3, CA3 region hippocampus; AC, anterior cingulate cortex; VH, ventral hippocampus; VC, visual cortex; MN, mammillary nucleus; AON, accessory olfactory nucleus.

Table 3 summarizes measured ether phospholipid concentration in whole brain, microsomal, and synaptosomal fractions. Values in the table are comparable to those previously reported in rat and mouse brain (1, 24). The brain microsomal fraction contained 8.3% of the total amount of brain ether phospholipids. The synaptosomal fraction contained 13.4%. Myelin (not shown) is reported to contain 41% of the whole brain PlsEtn, 17% of PlsCho, and 6% of plasmalyl-type phospholipids (1).

Calculations

Table 4 summarizes the values obtained by applying the operational equations outlined in the methods to experimental data. The change in the radioactivity of the individual ether phospholipids are given in column one and the "input functions" for *i* between T_1 and T_2 are given in column two. Column three gives the transfer coefficient ($k_{i-1 \rightarrow i}^*$). Column four gives the unlabeled ether phospholipid levels found in the microsomal fraction, and col-

umns five, six, and seven present the rate of synthesis, turnover rates, and half-lives, respectively.

The transfer coefficients ($k_{i-1 \rightarrow i}^*$) for hexadecanol incorporation into PakCho and PakEtn synthesis were 0.019 min^{-1} and 0.026 min^{-1} , respectively (Table 4). The calculated rates of synthesis of PakCho and PakEtn, each derived from PakOH (Fig. 1), equaled 1.2 and 9.3 $\text{nmol} \cdot \text{g}^{-1} \cdot \text{min}^{-1}$. The calculated transfer coefficients of PlsEtn and PlsCho were 0.030 and 0.046 min^{-1} , and resulted in synthesis rates for these phospholipids of 27.6 and 21.5 $\text{nmol} \cdot \text{g}^{-1} \cdot \text{min}^{-1}$. The approximate half-lives of the microsomal ether phospholipids were 36.5 min for PakCho, 26.7 min for PakEtn, 23.1 min for PlsEtn, and 15.1 min for PlsCho.

DISCUSSION

In this study, the incorporation of intravenously injected [1,1-³H]hexadecanol was used to identify differences between gray and white matter ether phospholipid metabolism in the adult rat, and to quantify the rate of synthesis, turnover and half-lives of brain microsomal ethanolamine and choline ether phospholipids in vivo. We also present a multicompartmental kinetic model, based on established pathways and known stoichiometry, to derive operational equations that were used to analyze the data.

Indeed, there is compelling evidence for heterogeneous brain ether phospholipid metabolism and concentration distribution. As stated, [1,1-³H]hexadecanol was selectively incorporated into gray matter ether phospholipids, as myelin radioactivity due to incorporation was always less than 10% of the total and only 3% at 240 min following infusion. Thus, in the adult rat, myelin ether phospholipids are relatively metabolically inactive and likely play a structural role. However, gray matter ether phospholipids are metabolically active consistent with their contribution to signal transduction and synaptic membrane turnover. Indeed, this type of developmental

TABLE 1. Regional brain radioactivity at different times following the intravenous infusion of 1.75 $\text{mCi} \cdot \text{kg}^{-1}$ [1,1-³H]hexadecanol in awake rats

Brain Region	Time After Start of Infusion		
	30 min	60 min	240 min
Gray matter regions			
Prefrontal	1,834 ± 489	1,626 ± 112	1,815 ± 255
Frontal	1,829 ± 432	1,952 ± 221	2,090 ± 183
Cingulate	1,914 ± 567	2,024 ± 202	3,135 ± 813
Motor	1,834 ± 525	1,870 ± 110	2,930 ± 815
Somatosensory	1,840 ± 509	1,859 ± 169	2,809 ± 626
Molecular layer	1,916 ± 551	2,089 ± 209	2,955 ± 776
CA1	1,644 ± 496	1,485 ± 102	1,880 ± 567
CA3	1,615 ± 507	1,477 ± 136	1,813 ± 460
Caudate putamen	1,812 ± 520	1,923 ± 254	1,751 ± 167
Thalamic nucleus	1,811 ± 527	1,817 ± 213	2,456 ± 364
White Matter Regions			
Corpus callosum	1,707 ± 513	656 ± 435	494 ± 520
External capsule	1,733 ± 497	763 ± 351	583 ± 459
Internal capsule	1,545 ± 564	791 ± 461	709 ± 748

Values are the means ± SD (n = 4) in units of $\text{dpm} \cdot \text{gram}^{-3}$.

TABLE 2. Radioactivity in different brain fractions following the 5 min infusion of 1.75 mCi·kg⁻¹ [1,1-³H]hexadecanol

Fraction	Time After Start of Infusion		
	30 min	60 min	240 min
Myelin	38,007 ± 7,817	18,746 ± 2,995	13,823 ± 9,707
Microsomal	38,717 ± 6,726	36,093 ± 9,562	46,818 ± 5,700
Synaptosomal	218,150 ± 11,561	129,955 ± 22,810	148,602 ± 14,759
Myelin			
16:0 (ol)	29,265 ± 2,470	13,797 ± 1,350	9,677 ± 664
PakOH	2,280 ± 874	1,856 ± 1,144	829 ± 318
PakEtn + PlsEtn	2,850 ± 1,102	1,593 ± 581	1,894 ± 567
PakCho + PlsCho	3,648 ± 1,596	1,500 ± 412	1,382 ± 263
Microsomes			
16:0 (ol)	21,217 ± 1,820	18,407 ± 2,093	15,824 ± 609
PakOH	2,517 ± 581	3,140 ± 1,335	4,026 ± 1,639
PakEtn + PlsEtn	8,324 ± 426	8,771 ± 2,057	17,416 ± 1,592
PakCho + PlsCho	6,659 ± 1,084	5,775 ± 1,047	9,597 ± 421
Synaptosomes			
16:0 (ol)	131,762 ± 9,380	50,422 ± 3,899	51,416 ± 1,912
PakOH	7,635 ± 5,236	7,018 ± 4,159	9,956 ± 6,687
PakEtn + PlsEtn	40,794 ± 3,709	42,105 ± 3,769	55,726 ± 7,133
PakCho + PlsCho	38,176 ± 6,108	30,409 ± 4,159	31,503 ± 2,080

Values are the means ± SD (n = 4) in units of dpm·g wet weight brain⁻¹.

regulation in the turnover of myelin has been demonstrated in rat studies measuring [¹⁴C]ethanolamine efflux and [¹⁴C]palmitate incorporation. In these studies, the half-life for PlsEtn as measured using [¹⁴C]ethanolamine. Efflux increased 12.5 fold between 20 days and 24 months of age, (53) indicative of the slower turnover of PlsEtn with increasing age. [¹⁴C]Palmitate incorporation in myelin also fell 4 fold between 20 and 38 days (54) consistent with the age-related decrease in myelin phospholipid turnover. Therefore the heterogeneous distribution of the tracer found in this study suggests that the myelin ether phospholipids of the adult rat maintains a structural role and those in the gray matter are involved in a more dynamic processes. The quantitative autoradiography supports this supposition since the differences between gray and white matter radioactivity following infusion rose to as high as 5:1 between 30 and 240 min (Table 1). Chemical analysis demonstrated, after subtracting unincorporated [1,1-³H]hexadecanol, myelin contained less than 10% of the net brain radioactivity between 30 and

240 min post-infusion and less than 3% at 240 min (Table 2). Others have also shown that the incorporation of radiolabeled precursors other than hexadecanol occur at different rates into myelin, mitochondria, microsomes, cytoplasm, neurons, and glia (26, 27, 55). Therefore, although exposed to equivalent levels of [1,1-³H]hexadecanol, myelin and gray matter ether phospholipids incorporated the tracer at markedly different rates into different spatial and chemical compartments. Thus, incorporation was not limited by availability of the tracer, but by the metabolism itself.

Under the steady state assumptions outlined in the Materials and Methods section, the calculated rate of synthesis of PakOH should be equal to the sum of the rates of synthesis of PakCho and PakEtn (equation 6). However the estimated synthesis rate of PakOH, using the integrated whole brain [1,1-³H]hexadecanol, was much less than predicted. Therefore, the labeled hexadecanol actually available for enzymic conversion to PakOH by alkyl dihydroxyacetonephosphate synthase (56, 57) was much lower than that found using whole brain measurements. Therefore, it is likely that following infusion most of the brain [1,1-³H]hexadecanol was partitioned into non-metabolically active membranes and was made unavailable for incorporation into PakOH by alkyl-DHAP synthase. The high octanol-water partition coefficient (log P_{hex} = 4.81) of hexadecanol and the cessation of the accumulation of brain PakOH radioactivity immediately following the end of infusion are consistent with this interpretation. Therefore, the lower than expected synthesis rate of PakOH formation calculated using equations 1a and 2 was most likely due to an overestimation of the specific activity of hexadecanol available for incorporation into PakOH as measured from whole brain extract. This will result in a lower than expected transfer coefficient for PakOH and as such a lower than expected rate of synthesis.

TABLE 3. Unlabeled ether phospholipid concentrations in rat whole brain and two of its membrane fractions

	Concentration		
	Whole Brain	Microsomes	Synaptosomes
Hexadecanol	4 ± 1	30 ± 4	1 ± 3
PakOH	351 ± 23	158 ± 15	22 ± 3
PakCho	401 ± 64	64 ± 14	174 ± 16
PakEtn	1,861 ± 237	361 ± 34	646 ± 30
PlsEtn	20,295 ± 1,710	922 ± 94	2,157 ± 142
PlsCho	823 ± 97	470 ± 53	183 ± 12
Total	23,732	1,975	3,182

Values are the means ± SD (n = 4) in units of nmol·g wet weight brain⁻¹.

TABLE 4. Transfer coefficients, synthesis rates, turnover rates, and half-life approximations of brain microsomal ether phospholipids

Compartment, <i>i</i>	$c_{br,i}^*$ (T_2)	$\int_{T_1}^{T_2} c_{br,i}^* dt$	$k_{i-1 \rightarrow i}^*$	$c_{br,i}^a$	$J_{i-1 \rightarrow i}$	F_i	$\tau_{1/2,i}$
	$dpm \cdot g^{-1}$	$dpm \cdot g^{-1} \cdot min^{-1}$	min^{-1}	$nmol \cdot g \text{ brain}^{-1}$	$nmol \cdot g^{-1} \cdot min^{-1}$	$\% min^{-1}$	min
PakOH	35,586 (5)	8.2×10^5		158	10.5 ^c	6.6 ^c	10.5 ^c
PakCho	15,811 (30)	3.0×10^5	0.019	64	1.2	1.9	36.5
PakEtn	21,068 (30)	4.6×10^5	0.026	361	9.3	2.6	26.7
PlsEtn	28,006 (30)	5.7×10^5	0.030 ^b	922	27.6	3.0	23.1
PlsCho	26,032 (30)	4.7×10^5	0.046	470	21.5	4.6	15.1

^a Concentration in microsomal fraction.

^b Corrected for loss of one [³H] atom from [1,1-³H]hexadecanol following the formation of PlsEtn from PakEtn.

^c Calculated using the steady-state restraint $J_{hex \rightarrow PakOH} = J_{PakOH \rightarrow PakCho} + J_{PakOH \rightarrow PakEtn}$ (equation 12).

Even though we were unable to directly determine the rate of PakOH formation using equation 2, the steady-state constraint of our model allowed us to indirectly make this calculation (equation 6). This value equaled 10.5 nmol·g⁻¹·min⁻¹ (Table 3). Because the specific activity of the purified alkyl-DHAP synthase is between 7.2–20.8 nmol·min⁻¹·mg⁻¹ protein (32), and alkyl-DHAP synthase activity in purified microsomes is approximately 65 nmol·min⁻¹·g⁻¹ (58), our values appear reasonable. Therefore, even though the direct measure of PakOH formation using whole brain measurements is invalid, due to the partitioning of the tracer into non-metabolically active membranes, the rate of synthesis of PakOH can be determined using this model.

The model also indicates that the microsomal rate of synthesis of PakEtn, PlsEtn, and PlsCho should equal each other under the steady-state conditions outlined in equation 7. As expected, the calculation using the ether phospholipid levels found in the microsomal fraction satisfies this prediction. These values were 9.3, 27.6, and 21.5 nmol·g⁻¹·min⁻¹, respectively. In this case, the rate of synthesis and the approximate turnover time of microsomal PlsEtn reported here is supported by experiments using tracer kinetic analysis (28) following an intracerebral injection of [1-³H]glycerol. The synthesis rate of PlsEtn in the 18-day-old rat is 32 nmol·g⁻¹·min⁻¹ (29). Thus, our rates for PakEtn, PakCho, PlsEtn, and PlsCho are very reasonable in comparison.

The half-lives of the microsomal ether phospholipid reported here are of the order of minutes. These short half-lives contrast with the reported half-lives of days to weeks that were determined by measuring radioactive efflux. Following labeling of brain ether phospholipids with [¹⁴C]ethanolamine, [³H]glycerol, [¹⁴C]choline, or [³²P]phosphate in the myelinating rat, the half-life in myelin and microsomal lipids was estimated as 11–58 days (27). With regard to PlsCho, using [³²P]phosphate, half lives of 30 days were reported for the whole brain, while the half-lives were 6 and 9.5 days for neurons and glia, respectively (26). The difference between short “incorporation” half-lives and the much longer “decay” half-lives likely reflects errors in the decay analysis due to recycling of the tracer, substantial back reactions, and partitioning of the tracer into phospholipids of stable non-metabolically active membranes (30). Errors due to tracer recycling and partitioning of the tracer into the phospholipids of stable, metabol-

ically inactive membranes are avoided in our calculations since only the initial rate of tracer accumulation is measured in the post-myelinating adult rat.

In summary, intravenously injected [1,1-³H]hexadecanol is rapidly incorporated into gray matter ether phospholipids in the adult rat brain by known pathways of biosynthesis. Incorporation into myelin compared with microsomes and synaptosomes is comparatively minimal, and the calculated microsomal synthesis rates of PakCho and PakEtn using this model are similar to the synthesis rates obtained in isolated rat brain microsomal preparations and those found using tracer kinetic analysis following labeled glycerol incorporation. Furthermore, we clearly demonstrate that there are several metabolically distinct brain ether phospholipid compartments in the brain and at least two major pools of plasmalogens. One is the static myelin pool, having a slow rate of tracer incorporation, and the other is a dynamic pool found in the gray matter. The rapid synthesis of microsomal ether lipids and the transfer of these phospholipids to synaptosomes are consistent with a dynamic role for ether phospholipids in brain signaling and neuroplasticity. **■**

Manuscript received 9 March 2001, in revised form 13 August 2001, and in re-revised form 4 October 2001.

REFERENCES

1. Ansell, G. B. 1973. Phospholipids and the nervous system. In *Form and Function of Phospholipids*. G. B. Ansell, J. N. Hawthorne and R. M. C. Dawson, editors. Elsevier, New York. 377–422.
2. Panganamala, R. V., L. A. Horrocks, J. C. Geer, and D. G. Cornwell. 1971. Positions of double bonds in the monounsaturated alk-1-enyl groups form the plasmalogens of human heart and brain. *Chem. Phys. Lipids*. **6**: 97–102.
3. Druilhet, R. E., M. L. Overturf, and W. M. Kirkendall. 1975. Structure of neutral glycerides and phosphoglycerides of human kidney. *Int. J. Biochem.* **6**: 893–901.
4. Blank, M. L., F. Snyder, L. W. Byers, B. Brooks, and E. E. Muirhead. 1979. Antihypertensive activity of an alkyl ether analog of phosphatidylcholine. *Biochem. Biophys. Res. Commun.* **90**: 1194–1200.
5. Horrocks, L. A. 1967. Composition of myelin from peripheral and central nervous system of the squirrel monkey. *J. Lipid Res.* **8**: 569–576.
6. Eng, L. F., and E. P. Noble. 1968. The maturation of rat brain myelin. *Lipids*. **3**: 157–162.
7. Choy, P. C., M. Skrzypczak, D. Lee, and F. T. Jay. 1997. Acyl-GPC and alkenyl/alkyl-GPC:acyl-CoA acyltransferases. *Biochim. Biophys. Acta*. **1348**: 124–133.
8. Yamashita, A., T. Sugiura, and K. Waku. 1997. Acyltransferases and

- transacylases involved in fatty acid remodeling of phospholipids and metabolism of bioactive lipids in mammalian cells. *J. Biochem.* **122**: 1–16.
9. Gunawan, J., M. Vierbuchen, and H. Debuch. 1979. Studies on the hydrolysis of 1-alk-1'-enyl-*sn*-glycero-3-phosphoethanolamine by microsomes from myelinating rat brain. *Hoppe-Seyler's Z. Physiol. Chem.* **360**: 971–978.
10. Gunawan, J., and H. Debuch. 1985. Alkenylhydrolase: a microsomal enzyme activity in rat brain. *J. Neurochem.* **44**: 370–375.
11. Van Iderstine, S. C., D. M. Byers, N. D. Ridgway, and H. W. Cook. 1996. Phospholipase D hydrolysis of plasmalogen and diacyl ethanolamine phosphoglycerides by protein kinase C dependent and independent mechanisms. *J. Lipid Med. Cell Signal* **15**: 175–192.
12. Farooqui, A. A., H. C. Yang, T. A. Rosenberger, and L. A. Horrocks. 1997. Phospholipase A₂ and its role in brain tissue. *J. Neurochem.* **69**: 889–901.
13. Hirashima, Y., A. A. Farooqui, J. S. Mills, and L. A. Horrocks. 1992. Identification and purification of calcium-independent phospholipase A₂ from bovine brain cytosol. *J. Neurochem.* **59**: 708–714.
14. Vierbuchen, M., J. Gunawan, and H. Debuch. 1979. Studies on the hydrolysis of 1-alkyl-*sn*-glycero-3-phosphoethanolamine in subcellular fractions of rat brain. *Hoppe-Seyler's Z. Physiol. Chem.* **360**: 1091–1097.
15. Feuerstein, G. Z. 1996. Platelet-activating factor: a case for its role in CNS function and brain injury. *J. Lipid Med. Cell Signal.* **14**: 109–114.
16. Izumi, T., and T. Shimizu. 1995. Platelet-activating factor receptor: gene expression and signal transduction. *Biochim. Biophys. Acta.* **1259**: 317–333.
17. Glaser, P. E., and R. W. Gross. 1994. Plasmenylethanolamine facilitates rapid membrane fusion: a stopped-flow kinetic investigation correlating the propensity of a major plasma membrane constituent to adopt an HII phase with its ability to promote membrane fusion. *Biochemistry.* **33**: 5805–5812.
18. Thai, T. P., C. Rodemer, A. Jauch, A. Hunziker, A. Moser, K. Gorgas, and W. W. Just. 2001. Impaired membrane traffic in defective ether lipid biosynthesis. *Hum. Mol. Genet.* **10**: 127–136.
19. Farooqui, A. A., H-C. Yang, and L. A. Horrocks. 1995. Plasmalogen, phospholipases A₂ and signal transduction. *Brain Res. Rev.* **21**: 152–161.
20. Zoeller, R. A., A. C. Lake, N. Nagan, D. P. Gaposchkin, M. A. Legner, and W. Lieberthal. 1999. Plasmalogens as endogenous antioxidants: somatic cell mutants reveal the importance of the vinyl ether. *Biochem. J.* **338**: 769–776.
21. Paltauf, F. 1994. Ether lipids in biomembranes. *Chem. Phys. Lipids.* **74**: 101–139.
22. Lee, T. C. 1998. Biosynthesis and possible biological functions of plasmalogens. *Biochim. Biophys. Acta.* **1394**: 129–145.
23. Radominska-Pyrek, A., and L. A. Horrocks. 1972. Enzymic synthesis of 1-alkyl-2-acyl-*sn*-glycero-3-phosphorylethanolamines by the CDP-ethanolamine: 1-acyl-2-acyl-*sn*-glycerol ethanolaminephosphotransferase from microsomal fraction of rat brain. *J. Lipid Res.* **13**: 580–587.
24. Sun, G. Y., and L. A. Horrocks. 1973. Metabolism of palmitic acid in the subcellular fractions of mouse brain. *J. Lipid Res.* **14**: 206–214.
25. Radominska-Pyrek, A., J. Strosznajder, Z. Dabrowiecki, G. Goracci, T. Chojnacki, and L. A. Horrocks. 1977. Enzymic synthesis of ether types of choline and ethanolamine phosphoglycerides by microsomal fractions from rat brain and liver. *J. Lipid Res.* **18**: 53–58.
26. Freysz, L., R. Bieth, and P. Mandel. 1969. Kinetics of the biosynthesis of phospholipids in neurons and glial cells isolated from rat brain cortex. *J. Neurochem.* **16**: 1417–1424.
27. Miller, S. L., J. A. Benjamins, and P. Morell. 1977. Metabolism of glycerophospholipids of myelin and microsomes in rat brain. Reutilization of precursors. *J. Biol. Chem.* **252**: 4025–4037.
28. Zilversmit, D. B., C. Entenman, and M. C. Fishler. 1942. On the calculation of "turnover time" and "turnover rate" from experiments involving the use of labeling agents. *J. Gen. Physiol.* **26**: 325–331.
29. Masuzawa, Y., T. Sugiura, Y. Ishima, and K. Waku. 1984. Turnover rates of the molecular species of ethanolamine plasmalogen of rat brain. *J. Neurochem.* **42**: 961–968.
30. Hennacy, D. M., and L. A. Horrocks. 1978. Recent developments in the turnover of proteins and lipids in myelin and other plasma membranes in the central nervous system. *Bull. Mol. Biol. Med.* **3**: 207–221.
31. Rapoport, S. I., D. Purdon, H. U. Shetty, E. Grange, Q. Smith, C. Jones, and M. C. Chang. 1997. In vivo imaging of fatty acid incorporation into brain to examine signal transduction and neuroplasticity involving phospholipids. *Ann. N.Y. Acad. Sci.* **820**: 56–74.
32. Hajra, A. K. 1995. Glycerolipid biosynthesis in peroxisomes (microbodies). *Prog. Lipid Res.* **34**: 343–364.
33. Washizaki, K., Q. R. Smith, S. I. Rapoport, and A. D. Purdon. 1994. Brain arachidonic acid incorporation and precursor pool specific activity during intravenous infusion of unesterified [³H]arachidonate in the anesthetized rat. *J. Neurochem.* **63**: 727–736.
34. Farooqui, A. A., S. I. Rapoport, and L. A. Horrocks. 1997. Membrane phospholipid alterations in Alzheimer's disease: deficiency of ethanolamine plasmalogens. *Neurochem. Res.* **22**: 523–527.
35. Whittaker, V. P. 1968. The morphology of fractions of rat forebrain synaptosomes separated on continuous sucrose density gradients. *Biochem. J.* **106**: 412–417.
36. Horrocks, L. A. 1969. Metabolism of the ethanolamine phosphoglycerides of mouse brain myelin and microsomes. *J. Neurochem.* **16**: 13–18.
37. Sun, G. Y., and L. A. Horrocks. 1970. The acyl and alk-1-enyl groups of the major phosphoglycerides from ox brain myelin and mouse brain microsomal, mitochondrial and myelin fractions. *Lipids.* **5**: 1006–1012.
38. Sun, A. Y., and T. Samorajski. 1970. Effects of ethanol on the activity of adenosine triphosphatase and acetylcholinesterase in synaptosomes isolated from guinea-pig brain. *J. Neurochem.* **17**: 1365–1372.
39. Sun, A. Y., G. Y. Sun, and T. Samorajski. 1971. The effect of phospholipase C on the activity of adenosine triphosphatase and acetylcholinesterase in synaptic membranes isolated from the cerebral cortex of squirrel monkey. *J. Neurochem.* **18**: 1711–1718.
40. Noronha, J. G., J. M. Bell, and S. I. Rapoport. 1990. Quantitative brain autoradiography of [9,10-³H]palmitic acid incorporation into brain lipids. *J. Neurosci. Res.* **26**: 196–208.
41. Folch, J., M. Lees, and G. H. Sloane-Stanley. 1957. A simple method for the isolation and purification of total lipides from animal tissue. *J. Biol. Chem.* **226**: 497–509.
42. Jolly, C. A., T. Hubbell, W. D. Behnke, and F. Schroeder. 1997. Fatty acid binding protein: stimulation of microsomal phosphatidic acid formation. *Arch. Biochem. Biophys.* **341**: 112–121.
43. Ansell, G. B., and S. Spanner. 1963. The alkaline hydrolysis of the ethanolamine plasmalogen of brain tissue. *J. Neurochem.* **10**: 941–945.
44. Rouser, G., A. N. Siakotos, and S. Fleischer. 1969. Quantitative analysis of phospholipids by thin-layer chromatography and phosphorus analysis of spots. *Lipids.* **1**: 85–86.
45. Breckenridge, W. C., and A. Kuksin. 1968. Specific distribution of short-chain fatty acids in molecular distillates of bovine milk fat. *J. Lipid Res.* **9**: 388–393.
46. Grange, E., J. Deutsch, Q. R. Smith, M. Chang, S. I. Rapoport, and A. D. Purdon. 1995. Specific activity of brain palmitoyl-CoA pool provides rates of incorporation of palmitate in brain phospholipids in awake rats. *J. Neurochem.* **65**: 2290–2298.
47. Robinson, P. J., J. Noronha, J. J. DeGeorge, L. M. Freed, T. Nariyai, and S. I. Rapoport. 1992. A quantitative method for measuring regional in vivo fatty-acid incorporation into and turnover within brain phospholipids: review and critical analysis. *Brain Res. Brain Res. Rev.* **17**: 187–214.
48. Rapoport, S. I., M. C. Chang, and A. A. Spector. 2001. Delivery and turnover of plasma-derived essential PUFAs in mammalian brain. *J. Lipid Res.* **42**: 678–685.
49. Reiner, J. M. 1953. The study of metabolic turnover rates by means of isotopic tracers. I. Fundamental relations. *Arch. Biochem. Biophys.* **46**: 53–79.
50. Rizzo, W. B., D. A. Craft, A. L. Dammann, and M. W. Phillips. 1987. Fatty alcohol metabolism in cultured human fibroblasts. Evidence for a fatty alcohol cycle. *J. Biol. Chem.* **262**: 17412–17419.
51. Hansch, L. A., and D. Elkins. 1971. Partition coefficients and their uses. *Chem. Rev.* **71**: 525–616.

52. Spector, A. A., and J. M. Soboroff. 1972. Studies on the cellular mechanism of free fatty acid uptake using an analog, hexadecanol. *J. Lipid Res.* **13**: 790–796.
53. Porcellati, G., G. Goracci, and G. Arienti. 1983. Lipid turnover. In *Handbook of Neurochemistry*. A. Lajtha, editor. Plenum Press, New York. 277–310.
54. Tabata, H., J. M. Bell, J. C. Miller, and S. I. Rapoport. 1986. Incorporation of plasma palmitate into the brain of the rat during development. *Brain Res.* **394**: 1–8.
55. Mandel, P., and J. L. Nussbaum. 1966. Incorporation of ^{32}P into the phosphatides of myelin sheaths and of intracellular membranes. *J. Neurochem.* **13**: 629–642.
56. Snyder, F. 1972. Ether-linked lipids and fatty alcohol precursors in neoplasms. In *Ether Lipids: Chemistry and Biology*. F. Snyder, editor. Academic Press, New York. 273–295.
57. de Vet, E. C., Y. H. Hilkes, M. W. Fraaije, and H. van den Bosch. 2000. Alkyl-dihydroxyacetonephosphate synthase: presence and role of flavin adenine dinucleotide. *J. Biol. Chem.* **275**: 6276–6283.
58. Brown, A. J., and F. Snyder. 1983. The mechanism of alkyl-dihydroxyacetone-P synthase: formation of [^3H]H $_2\text{O}$ from acyl[1-R- ^3H]-dihydroxyacetone-P by purified alkyl-dihydroxyacetone-P synthase in the absence of acylhydrolase activity. *J. Biol. Chem.* **258**: 4184–4189.